International Journal of Applied Pharmaceutics

ISSN- 0975-7058 Vol 16, Issue 6, 2024

Original Article

NOVEL HYBRIDS OF QUINOLINE LINKED PYRIMIDINE DERIVATIVES AS CYCLOOXYGENASE INHIBITORS: MOLECULAR DOCKING, ADMET STUDY, AND MD SIMULATION

DEEPTHI K.[1], MANJUNATH S. KATAGI[2], JENNIFER FERNANDES[1*], SHESHAGIRI DIXIT[3], DEEPSHIKHA SINGH[4]

[1]Department of Pharmaceutical Chemistry, NGSM Institute of Pharmaceutical Sciences, Nitte (Deemed to be University), Mangalore-575018, Karnataka, India. [2]Department of Pharmaceutical Chemistry, Bapuji Pharmacy College, Rajiv Gandhi University of Health Sciences, Davanagere-577004, Karnataka, India. [3]Computer Aided Drug Design Laboratory, Department of Pharmaceutical Chemistry, JSS College of Pharmacy Mysore, JSS Academy of Higher Education and Research, Mysore-570015, Karnataka, India. [4]Department of Pharmaceutical Chemistry, JSS College of Pharmacy Mysore, JSS Academy of Higher Education and Research, Mysore-570015, Karnataka, India

[*]Corresponding author: Jennifer Fernandes; [*]Email: fernandesj@nitte.edu.in

Received: 10 Jul 2024, Revised and Accepted: 31 Aug 2024

ABSTRACT

Objective: Finding novel anti-inflammatory compounds is a crucial sector of research despite the significant advances this field has made. Inefficiency and unfavorable side effects are indeed potential drawbacks of conventional therapy utilizing steroidal or nonsteroidal drugs. This study aims to screen the designed quinoline-linked pyrimidine derivatives as Cyclooxygenase (COX) inhibitors.

Methods: In the present study, we assessed the binding interactions of designed quinoline-linked pyrimidine derivatives with COX enzymes using a molecular docking approach. Using Molecular Dynamics (MD) simulations, the compound's behavior was further investigated and its stability and conformational dynamics were demonstrated. Schrödinger's QikProp program was utilized to analyze the Absorption, Distribution, Metabolism, and Excretion (ADME) properties and toxicity properties were further investigated using Osiris Property Explorer. Additionally, the protein-ligand complexes' binding free energy has been ascertained using the Molecular Mechanics/Generalized Born Surface Area (MM-GBSA) approach, which offered crucial information regarding the strength of their interactions.

Results: The designed quinoline-linked pyrimidine derivatives fulfilled the Lipinski Rule of Five and had physicochemical characteristics within acceptable ranges, better ADME properties, and were non-toxic. Among the designed compounds, QPDU1 and QPDT6 showed correspondingly good docking scores for COX-1 and COX-2. QPDT6 was additionally analyzed by MD simulation studies to thoroughly examine the interaction between protein and ligand and their stability.

Conclusion: The proposed compounds exhibit strong binding affinities to COX enzymes, stable interactions in MD simulations, and favorable drug-like features. These results support the need for more research and development of these substances as possible anti-inflammatory drugs.

Keywords: Quinoline, Pyrimidine, Cyclooxygenase, Molecular docking, Molecular dynamics

DOI: https://dx.doi.org/10.22159/ijap.2024v16i6.52023 Journal homepage: https://innovareacademics.in/journals/index.php/ijap

INTRODUCTION

Heterocyclic chemistry is vital in the design, synthesis, and optimization of potential pharmaceutical agents. The vast majority of commercially available drugs contain one or more heterocyclic rings. Heterocycles not only serve as an active pharmaceutical ingredient but also as key intermediates in chemical synthesis, enabling the development of new drug leads and analogs. The exploration of diverse heterocyclic scaffolds continues to be an active area of research for discovering novel therapeutic agents. Heterocycles are indispensable in the development and discovery of drugs due to their biological activity and versatility. Their incorporation into drug molecules contributes to the advancement of medicine by providing effective treatments for various diseases and conditions [1]. Quinoline is a bicyclic heterocyclic ring that contains nitrogen and is fused with pyridine at the benzene ring. Quinoline is referred to as 1-aza naphthalene or benzo [*b*] pyridine [2]. Quinoline is an important molecule commonly present in natural products showing a broad range of biological activity [3]. It has been observed that quinoline derivatives show a wide spectrum of biological functions comprising antibacterial [4], anti-malarial [5], antileishmanial activity[6], anti-cancer activity [7], anti-inflammatory [8], antioxidant [9], anti-tubercular [10], anti-viral [11], anti-fungal [12], anti-HIV [13], antidepressant activity [14], anticonvulsant [15], antidiabetic [16], hypocholesterolaemia activity [17], analgesic [18], anti-alzheimer's [19], and antiulcer activity [20]. Pyrimidine is a nitrogen-containing six-membered heterocyclic aromatic compound. Heterocycles containing pyrimidines represent a significant class of both synthetic and natural substances, with several applications in medicine and advantageous biological characteristics [21]. According to reports, pyrimidine derivatives exhibit anti-inflammatory [22], antimicrobial activity [23], anticancer [24], anti-HIV activity [25], antiplatelet [26], antihypertensive [27], antiviral [28], antifungal [29], anti-Alzheimer's [30], antidiabetic [31], antitubercular [32], antioxidant [33], antidepressant [34], analgesic [35], anticonvulsant [36], anti-Parkinson [37], and antihyperlipidemic activity [38].

Inflammation is the body's defense mechanism that fights against dangerous stimulants that harm tissues and cells; however, unrestricted inflammation is the primary factor behind some illnesses, including allergies, cardiovascular diseases, cancer, and autoimmune disorders [39]. The complex biological process of inflammation includes the activation of immune cells, the release of signaling molecules, and changes in blood flow. Eliminating the source of cell injury, removing damaged cells and tissues, and starting tissue repair are the main purposes of inflammation. In the context of acute inflammation, the body's response is typically well-regulated and aims to resolve the issue efficiently. This acute inflammatory response is essential for maintaining overall health and has a significant impact on defending the body against infections and injuries. However, when the inflammatory process is not properly regulated or if the initial cause of inflammation persists, it can lead to chronic inflammation [40]. Prostaglandins are lipid compounds that are essential to the process of inflammation. They are created by the cells in the body through a series of enzymatic reactions, with the Cyclooxygenase (COX) enzyme being an important player in this process [41]. Mammals contain two catalytically functional COX isoforms, COX-1 and COX-2. There are significant parallels between the COX-1 and COX-2 protein

sequences, as well as in their catalytic mechanisms. Both isoforms take part in converting arachidonic acid into prostaglandins [42]. Non-steroidal anti-inflammatory Drugs (NSAIDs) are in general, given as analgesics, anti-inflammatories, and antipyretics. NSAIDs function by blocking the COX enzymes, which lowers the amount of prostaglandins that are produced [43].

Even though this discipline has achieved substantial progress, finding novel anti-inflammatory compounds is still an essential field of study. Conventional medical care using steroidal or nonsteroidal agents may indeed have limitations, such as inefficiency and undesirable side effects. That's why scientists and researchers are constantly exploring innovative approaches to discover safer and more effective anti-inflammatory compounds. This enables the development of novel compounds that specifically target inflammatory pathways, minimizing side effects and maximizing therapeutic benefits [44]. We have performed *in silico* studies to screen the inhibitory effect of designed quinoline-linked pyrimidine derivatives on COX enzymes.

MATERIALS AND METHODS

Docking studies

The *in silico* analysis was performed on Maestro version 13.5.128, MMshare Version 6.1.128, Release 2023-1, with Linux-x86_64 operating system.

Ligand preparation

Chemical structures of compounds are designed using ChemDraw, and then their structures are converted to SMILES format. The SMILES representations of the designed compounds are then imported into Schrödinger. The Schrödinger module LigPrep (https://www.schrodinger.com/platform/products/ligprep/) is used for ligand preparation. It neutralizes charged groups in the ligands by adding or removing hydrogen ions. This step is necessary before ionization states can be generated. It removes extra molecules, such as counter ions in salts and water molecules, to obtain a clean and representative structure of the ligand. LigPrep eliminates different tautomeric forms of a molecule. The prepared ligands in 2D structures are converted to 3D structures [45].

Protein preparation

The X-ray crystal structures for the COX-2 and COX-1 enzymes were taken from the Protein Data Bank (PDB) (https://www.rcsb.org/) with PDB IDs of 5IKR and 6Y3C, correspondingly. The protein structures were imported and processed using Schrödinger's Protein Preparation Wizard. Preprocessing includes assignments of bond orders and formal charges, correction of bond order errors, and addition of missing atoms. Carried out the protein structural optimization. Refinement of bond lengths, angles, and torsion angles might be essential to provide a more realistic depiction of the original structure. Eliminated water molecules from the structure of the protein. To streamline the system and concentrate on the ways that ligands and proteins interact, this phase is important. The protein's energy was minimized to produce a stable shape. Finding a low-energy state entails modifying the atomic locations during minimization. To further enhance its quality, the protein's structure was further improved. This stage could involve more refinement or optimization to improve the protein model's accuracy. The most pertinent ionization state was selected once the ionization states of amino acid residues were determined. To create a grid for molecular docking, Receptor Grid Generation Wizard was utilized. To do this, a 3D grid must be defined around the protein's active region, where ligands are to be docked [46].

Molecular docking

The ligand is docked into the protein binding site using the Glide docking technique (https://www.schrodinger.com/platform/products/glide/). Glide assesses and ranks various ligand poses according to their expected binding affinities using a scoring algorithm. How the protein and ligand interact is evaluated by the scoring function. We analyze docking poses in the Extra-Precision mode (XP mode). The program examines many interactions, such as steric conflicts, metal-ligation interactions, hydrophobic interactions, and hydrogen bonding. This stage sheds light on the characteristics of the interactions between ligands and proteins. The Glide Score function is used for the final scoring [47].

Molecular mechanics/Generalized born surface area (MM-GBSA)

Protein-ligand complex binding free energy is estimated using Prime MM-GBSA (https://www.schrodinger.com/platform/products/prime/). It computes the energy changes related to ligand binding to a protein receptor by combining continuum solvation models with force fields from molecular mechanics. The binding free energy, or ΔG bind, is determined by deducting the complex's energy from the energies of the separated protein and ligand after considering any entropy contributions and the solvation-free energy [48].

ADMET studies

Schrödinger's QikProp (https://www.schrodinger.com/platform/products/qikprop/) tool is designed to anticipate different physicochemical and ADME features of organic compounds. The abbreviation ADME refers to the processes of absorption, distribution, metabolism, and excretion—all important elements in comprehending how drug-like compounds behave within the human body. Numerous physicochemical parameters, like molecular weight, hydrogen bond donors and acceptors, lipophilicity (log P), Polar Surface Area (PSA), and more, can be computed using QikProp. The program makes predictions for characteristics of ADME, including oral absorption in humans, blood-brain barrier penetration, and aqueous solubility, among others. The molecules' Three-Dimensional (3D) structure, which accounts for their structural characteristics and conformational flexibility, is the basis for the predictions [49]. The toxicity and drug-likeness of the designed quinoline-linked pyrimidine derivatives were determined by using the OSIRIS property explorer (https://www.organic-chemistry.org/prog/peo). To calculate various drug-relevant properties, OSIRIS Property Explorer uses chemical structures. Color codes and values are used to express the results. C log P, solubility, drug score, drug-likeness and toxicity parameters such as tumorigenic, mutagenicity, reproductive effect, and irritant effect are some of the properties analyzed [50].

Molecular dynamics (MD) simulation studies

Among the designed compounds, QPDT6 showed the highest docking score and it is further analyzed by MD simulation studies. The Schrödinger LLC software was used to do MD simulations to analyze compound QPDT6. The duration of these simulations was 100 nanoseconds, generating 1000 frames at 20 picosecond intervals. The SPC model was utilized to achieve solvation while the system was kept under orthorhombic boundary conditions. To verify the neutrality of the systems, the charges on the models were neutralized by the introduction of sodium and chloride ions. The box size was determined using a buffering technique, and the systems underwent 2000 energy reduction iterations with a convergence threshold of 25 kcal mol−1A°−1. Following energy minimization, simulations using the NPT ensemble were run at 300 Kelvin temperature and 1 bar pressure [51].

RESULTS

In silico studies were carried out for designed quinoline-linked pyrimidine derivatives. QPDG, QPDU, and QPDT are the three series of compounds that were designed. Table 1 illustrates the structures of designed compounds from each series.

Physicochemical properties

The physicochemical properties of the designed compounds are listed in table 2. There are no violations of Lipinski's rule of five, and the values of all the compounds are within the recommended limit.

ADMET properties

ADME properties of designed quinoline derivatives are determined by the Qikprop module of Schrödinger and it is given in table 3.

Table 1: Structures of designed quinoline-linked pyrimidine derivatives

QPDG series		QPDU series		QPDT series	
Ligand ID	**Structure**	**Ligand ID**	**Structure**	**Ligand ID**	**Structure**
QPDG1	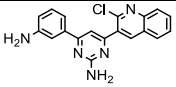	QPDU1	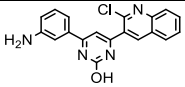	QPDT1	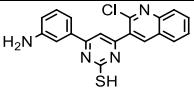
QPDG2	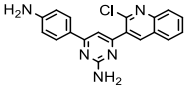	QPDU2	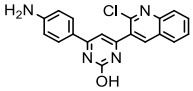	QPDT2	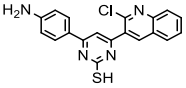
QPDG3	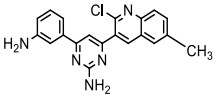	QPDU3	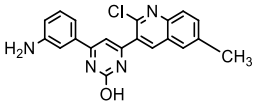	QPDT3	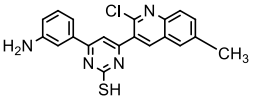
QPDG4	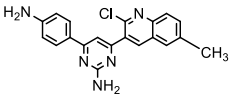	QPDU4	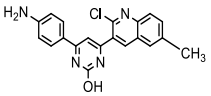	QPDT4	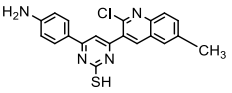
QPDG5	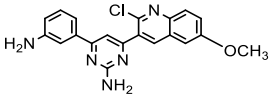	QPDU5	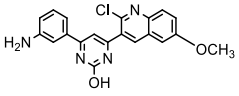	QPDT5	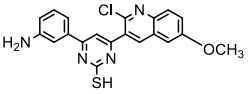
QPDG6	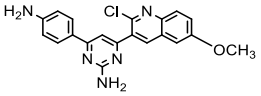	QPDU6	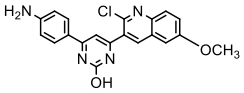	QPDT6	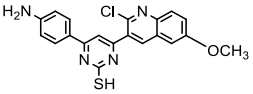
QPDG7	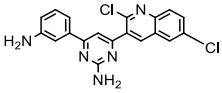	QPDU7	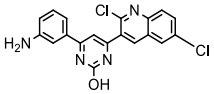	QPDT7	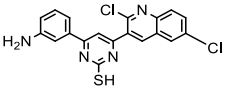
QPDG8	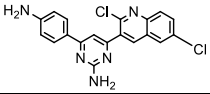	QPDU8	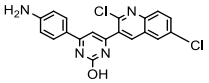	QPDT8	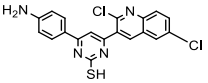

Table 2: Physicochemical properties of quinoline-linked pyrimidine derivatives

Ligand ID	Molecular weight	QPlogPo/w	Donor HB	Accpt HB	Rule of five
QPDG1	347.806	3.108	3.5	4.5	0
QPDG2	347.806	3.104	3.5	4.5	0
QPDG3	361.833	3.4	3.5	4.5	0
QPDG4	361.833	3.399	3.5	4.5	0
QPDG5	377.832	3.225	3.5	5.25	0
QPDG6	377.832	3.227	3.5	5.25	0
QPDG7	382.251	3.587	3.5	4.5	0
QPDG8	382.251	3.587	3.5	4.5	0
QPDU1	348.791	3.499	2.5	4	0
QPDU2	348.791	3.496	2.5	4	0
QPDU3	362.818	3.802	2.5	4	0
QPDU4	362.818	3.799	2.5	4	0
QPDU5	378.817	3.611	2.5	4.75	0
QPDU6	378.817	3.612	2.5	4.75	0
QPDU7	383.236	3.984	2.5	4	0
QPDU8	383.236	3.985	2.5	4	0
QPDT1	364.851	4.486	2.3	4	0
QPDT2	364.851	4.483	2.3	4	0
QPDT3	378.878	4.787	2.3	4	0
QPDT4	378.878	4.788	2.3	4	0
QPDT5	394.878	4.596	2.3	4.75	0
QPDT6	394.878	4.597	2.3	4.75	0
QPDT7	399.297	4.976	2.3	4	0
QPDT8	399.297	4.973	2.3	4	0
Anthrafenine	588.551	8.031	0	5.500	2
Epirizole	234.257	3.082	0	3.000	0

Molecular docking

The designed quinoline-linked pyrimidine derivatives were placed for molecular docking analysis with two COX enzymes, and the interactions between the enzyme and compounds were analyzed. The docking scores were compiled in table 5 for COX-1 and COX-2 enzymes with PDB ID 6Y3C and 5IKR correspondingly. 2D and 3D interaction of designed quinoline-linked pyrimidine derivatives with enzymes COX-2 and COX-1 was given in fig. 1 and fig. 2, respectively.

MM-GBSA

The ligand binding free energy (ΔG bind) of docked molecules was predicted using the Prime MM-GBSA technique and presented in the corresponding table 6 and table 7 for COX-2 and COX-1, respectively.

Table 3: ADME properties of quinoline-linked pyrimidine derivatives

Ligand ID	%HOA[a]	QPPCaco[b]	Qplog Khsa[c]	Qplog BB[d]	QPlog HERG[e]	QPPMDCK[f]
QPDG1	88.655	269.894	0.26	-1.197	-6.442	254.947
QPDG2	88.571	267.811	0.26	-1.201	-6.437	252.132
QPDG3	90.369	270.043	0.404	-1.243	-6.351	254.556
QPDG4	90.311	268.235	0.404	-1.247	-6.35	252.612
QPDG5	89.34	269.762	0.294	-1.297	-6.324	254.286
QPDG6	89.296	267.979	0.296	-1.301	-6.327	252.676
QPDG7	91.469	270.099	0.365	-1.057	-6.352	628.505
QPDG8	91.408	268.094	0.366	-1.061	-6.353	623.362
QPDU1	91.627	294.607	0.419	-1.153	-6.433	280.381
QPDU2	91.561	292.725	0.419	-1.156	-6.429	277.918
QPDU3	93.405	294.744	0.571	-1.199	-6.347	280.566
QPDU4	93.336	292.883	0.571	-1.201	-6.344	278.141
QPDU5	92.279	294.55	0.447	-1.252	-6.315	279.524
QPDU6	92.241	292.802	0.448	-1.255	-6.318	278.015
QPDU7	94.475	294.805	0.529	-1.012	-6.344	691.179
QPDU8	94.43	292.949	0.53	-1.016	-6.346	687.079
QPDT1	100	1160.359	0.518	-0.333	-6.532	3536.192
QPDT2	100	1152.066	0.518	-0.336	-6.528	3500.718
QPDT3	100	1160.248	0.671	-0.361	-6.435	3526.456
QPDT4	100	1152.789	0.672	-0.364	-6.437	3504.98
QPDT5	100	1159.294	0.544	-0.417	-6.411	3524.533
QPDT6	100	1151.81	0.545	-0.421	-6.414	3502.382
QPDT7	100	1160.659	0.631	-0.179	-6.444	8731.041
QPDT8	100	1152.734	0.631	-0.182	-6.44	8647.378
Anthrafenine	100	655.728	1.764	0.413	-8.760	6685.361
Epirizole	100	4946.865	0.109	0.158	-4.249	2785.086

[a]Percent human oral absorption, [b]Apparent caco-2 cell permeability, [c]Binding to human serum albumin, [d]Brain/blood partition coefficient, [e]Blockage of HERG K+channels, [f]Apparent MDCK cell permeability.

The toxicity calculations and drug-relevant properties of designed quinoline-linked pyrimidine derivatives were determined using Osiris property explorer and it is given in table 4.

Table 4: Toxicity calculation Drug likeness/scores of quinoline-linked pyrimidine derivatives based on Osiris property explorer

Drug-relevant properties					Toxicity			
Ligand ID	C log P	Solubility	Drug likeness	Drug score	Tumorigenic	Reproductive effect	Irritant effect	Mutagenicity
QPDG1	3.63	-5.80	-3.42	0.43	Green	Green	Green	Green
QPDG2	3.63	-5.80	-0.97	0.53	Green	Green	Green	Green
QPDG3	3.97	-6.14	-4.40	0.40	Green	Green	Green	Green
QPDG4	3.97	-6.14	-1.97	0.45	Green	Green	Green	Green
QPDG5	3.56	-5.81	-2.73	0.43	Green	Green	Green	Green
QPDG6	3.56	-5.81	-0.41	0.57	Green	Green	Green	Green
QPDG7	4.24	-6.53	-2.48	0.41	Green	Green	Green	Green
QPDG8	4.24	-6.53	-0.18	0.55	Green	Green	Green	Green
QPDU1	3.96	-5.42	-3.34	0.42	Green	Green	Green	Green
QPDU2	3.96	-5.42	-0.92	0.52	Green	Green	Green	Green
QPDU3	4.31	-5.77	-4.32	0.39	Green	Green	Green	Green
QPDU4	4.31	-5.77	-1.92	0.43	Green	Green	Green	Green
QPDU5	3.89	-5.44	-2.67	0.42	Green	Green	Green	Green
QPDU6	3.89	-5.44	-0.36	0.56	Green	Green	Green	Green
QPDU7	4.57	-6.16	-2.50	0.39	Green	Green	Green	Green
QPDU8	4.57	-6.16	-0.19	0.53	Green	Green	Green	Green
QPDT1	4.12	-6.32	-5.64	0.39	Green	Green	Green	Green
QPDT2	4.12	-6.32	-3.21	0.41	Green	Green	Green	Green
QPDT3	4.47	-6.67	-6.62	0.37	Green	Green	Green	Green
QPDT4	4.47	-6.67	-4.21	0.37	Green	Green	Green	Green
QPDT5	4.05	-6.34	-4.96	0.39	Green	Green	Green	Green
QPDT6	4.05	-6.34	-2.65	0.41	Green	Green	Green	Green
QPDT7	4.73	-7.06	-4.76	0.35	Green	Green	Green	Green
QPDT8	4.73	-7.06	-2.46	0.37	Green	Green	Green	Green
Antrafenine	6.39	-6.43	0.49	0.07	Red	Red	Green	Red
Epirizole	1.26	0.19	2.81	0.94	Green	Green	Green	Green

MD simulation

Based on the docking score, the compound QPDT6 was selected from the designed molecules for further MD simulation investigation. MD simulation was run for 100 ns on an explicit hydration environment to evaluate compound QPDT6's stability in a complex with 5IKR. Root mean Square Deviation (RMSD), Root mean Square Fluctuation (RMSF), protein-ligand contact mapping, and ligand-protein contacts were used to assess the MD simulation data. Throughout the trajectory analysis, the average displacement of a set of atoms in

each frame concerning a reference frame is measured using the RMSD, which sheds light on structural changes with time. Tracking the protein's RMSD during the simulation can reveal details about structural conformation. Ligand RMSD reflects the stability of the ligand with the protein and its binding pocket (fig. 3A). The RMSF is valuable for identifying local variations along the protein chain (fig. 3B). Interactions between the enzyme 5IKR and the ligand QPDT6 can be tracked throughout the simulation. The 'Simulation Interactions Diagram' panel allows for the exploration of more detailed subtypes within each interaction type (fig. 3C). A schematic of detailed interactions of atoms of QPDT6 with the 5IKR residues is given in fig. 3D.

Table 5: Glide docking scores (kcal mol−1) of the quinoline-linked pyrimidine derivatives on enzymes COX-2 (PDB ID: 5IKR) and COX-1 (PDB ID: 6Y3C)

Ligand ID	Docking score (kcal mol^{-1})	
	COX-2	COX-1
QPDG1	-6.698	-6.410
QPDG2	-6.923	-6.137
QPDG3	-7.026	-6.844
QPDG4	-6.772	-6.981
QPDG5	-6.695	-7.050
QPDG6	-6.874	-6.460
QPDG7	-6.163	-6.469
QPDG8	-6.511	-2.836
QPDU1	-6.303	-7.483
QPDU2	-6.239	-6.632
QPDU3	-6.764	-6.715
QPDU4	-6.778	-7.157
QPDU5	-6.699	-6.970
QPDU6	-7.366	-6.721
QPDU7	-6.795	-6.958
QPDU8	-6.717	-5.636
QPDT1	-6.428	-6.630
QPDT2	-6.819	-6.869
QPDT3	-5.905	-6.612
QPDT4	-6.593	-7.104
QPDT5	-6.647	-7.132
QPDT6	-7.609	-5.624
QPDT7	-6.768	-6.815
QPDT8	-6.534	-6.955
Anthrafenine	-6.798	-7.127
Epirizole	-4.632	-5.318

Table 6: MM-GBSA for quinoline-linked pyrimidine derivatives with COX-2

Ligand ID	ΔG Bind (kcal mol^{-1})[a]	ΔG Bind Coulomb[b]	ΔG Bind Covalent[c]	ΔG Bind Hbond[d]	ΔG Bind lipophilic[e]	ΔG Bind van der[f]
QPDG1	-25.89	-1.61	2.87	-1.03	-32.79	-37.82
QPDG2	-40.71	-9.99	2.38	-1.59	-23.91	-44.46
QPDG3	-58.80	-14.26	2.36	-2.42	-30.75	-44.48
QPDG4	-27.22	-5.30	1.68	-1.71	-23.88	-42.55
QPDG5	-44.40	-9.60	-0.20	-1.09	-25.29	-46.86
QPDG6	-44.81	-12.51	1.87	-1.77	-24.91	-46.00
QPDG7	-28.35	-1.27	1.34	-0.95	-25.64	-43.49
QPDG8	-29.33	-2.69	2.64	-1.61	-25.43	-43.31
QPDU1	-28.62	1.92	0.86	-0.23	-33.56	-37.76
QPDU2	-49.94	-13.39	5.96	-1.95	-29.25	-44.99
QPDU3	-59.22	-14.96	2.29	-2.52	-30.78	-44.28
QPDU4	-28.16	-6.52	1.58	-0.97	-23.71	-43.33
QPDU5	-43.14	-9.43	0.07	-0.43	-25.13	-46.52
QPDU6	-44.81	-13.82	2.31	-1.15	-24.07	-45.53
QPDU7	-65.22	-13.68	2.45	-2.54	-34.49	-44.36
QPDU8	-30.60	-6.41	1.63	-0.97	-24.94	-43.18
QPDT1	-56.64	-14.59	2.50	-2.28	-24.56	-42.16
QPDT2	-42.44	-8.03	1.95	-0.91	-24.35	-46.13
QPDT3	-43.48	-5.17	-0.02	-0.19	-26.96	-47.51
QPDT4	-37.20	-16.01	1.22	-2.17	-20.29	-34.18
QPDT5	-45.43	-7.34	-0.11	-0.38	-25.93	-47.94
QPDT6	-45.55	-9.33	1.55	-1.10	-25.37	-47.90
QPDT7	-67.67	-12.98	3.11	-2.34	-34.14	-45.55
QPDT8	-39.55	-15.07	1.23	-2.15	-21.46	-34.42
Epirizole	-44.74	-10.82	3.57	-0.30	-22.53	-32.17
Antrafenine	-40.67	-17.33	10.04	-1.10	-27.80	-47.61

[a]Free energy of binding, [b]Coulomb energy, [c]Covalent energy, [d]Hydrogen bonding energy, [e]Hydrophobic energy, [f]Van der waals energy

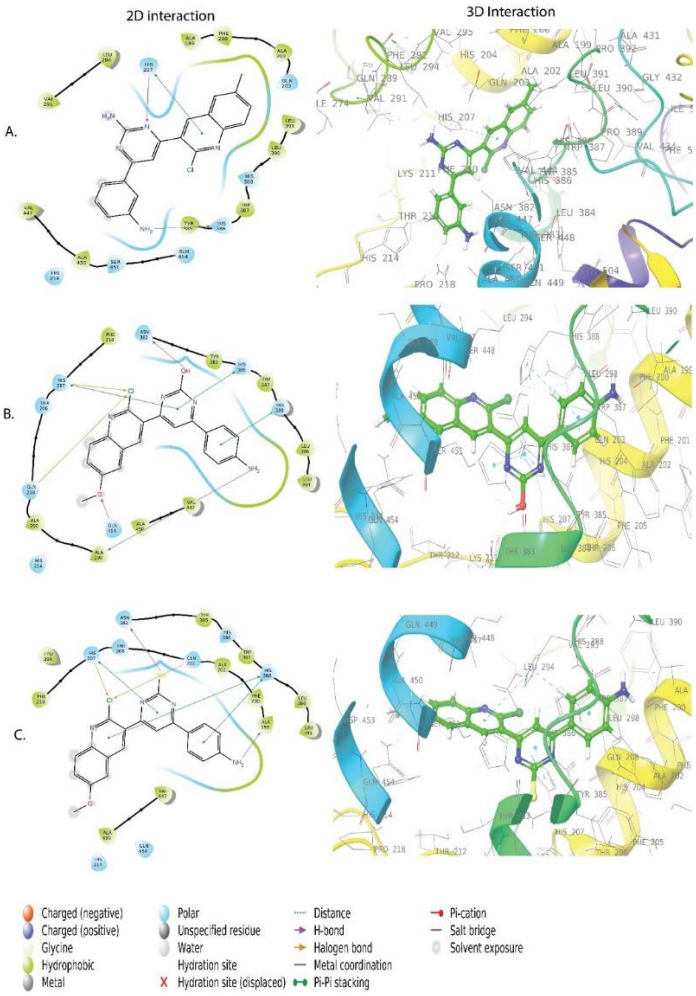

Fig. 1: 2D and 3D interaction of compound (A) QPDG3 with 5IKR, (B) QPDU6 with 5IKR, (C) QPDT6 with 5IKR

Table 7: MM-GBSA for quinoline-linked pyrimidine derivatives with COX-1

Ligand ID	ΔG Bind (kcal mol^{-1})[a]	ΔG Bind Coulomb[b]	ΔG Bind Covalent[c]	ΔG Bind H bond[d]	ΔG Bind lipophilic[e]	ΔG Bind van der[f]
QPDG1	-67.14	-11.53	2.87	-3.68	-28.44	-43.52
QPDG2	-68.51	-13.01	3.62	-5.24	-28.40	-43.73
QPDG3	-66.71	-13.74	4.28	-3.49	-34.34	-44.31
QPDG4	-66.61	-14.47	5.31	-5.50	-34.05	-43.36
QPDG5	-66.77	-13.07	3.33	-3.53	-32.85	-42.91
QPDG6	-68.29	-14.34	4.60	-5.49	-32.99	-41.65
QPDG7	-72.79	-9.87	4.34	-3.50	-38.27	-45.42
QPDG8	-73.85	-11.47	5.01	-5.48	-37.98	-44.54
QPDU1	-68.99	-19.11	2.82	-2.58	-28.41	-42.22
QPDU2	-69.05	-15.94	3.47	-5.35	-28.44	-43.61
QPDU3	-68.60	-17.25	4.22	-3.55	-34.36	-44.09
QPDU4	-68.44	-17.96	5.14	-5.60	-34.15	-43.13
QPDU5	-68.26	-16.29	3.33	-3.58	-32.88	-42.72
QPDU6	-68.79	-18.54	4.76	-5.57	-33.11	-41.35
QPDU7	-74.74	-13.93	4.24	-3.61	-38.28	-45.14
QPDU8	-75.44	-14.93	4.93	-5.59	-38.03	-44.40
QPDT1	-65.40	-12.30	3.32	-3.67	-29.12	-44.28
QPDT2	-70.82	-13.69	3.43	-5.24	-28.34	-44.87
QPDT3	-68.94	-14.16	4.12	-3.45	-34.18	-45.52
QPDT4	-67.58	-12.07	5.94	-5.30	-34.54	-45.03
QPDT5	-69.57	-13.97	3.27	-3.52	-32.82	-44.09
QPDT6	-70.17	-16.03	4.74	-5.51	-32.98	-42.72
QPDT7	-74.74	-7.44	3.03	-3.58	-36.77	-45.34
QPDT8	-75.94	-12.16	4.65	-5.47	-37.79	-45.73
Antrafenine	-55.56	-2.84	4.12	-0.22	-37.37	-60.74
Epirizole	-46.24	-11.56	1.84	-0.91	-21.76	-33.71

[a]Free energy of binding, [b]Coulomb energy, [c]Covalent energy, [d]Hydrogen bonding energy, [e]Hydrophobic energy, [f]Van der waals energy

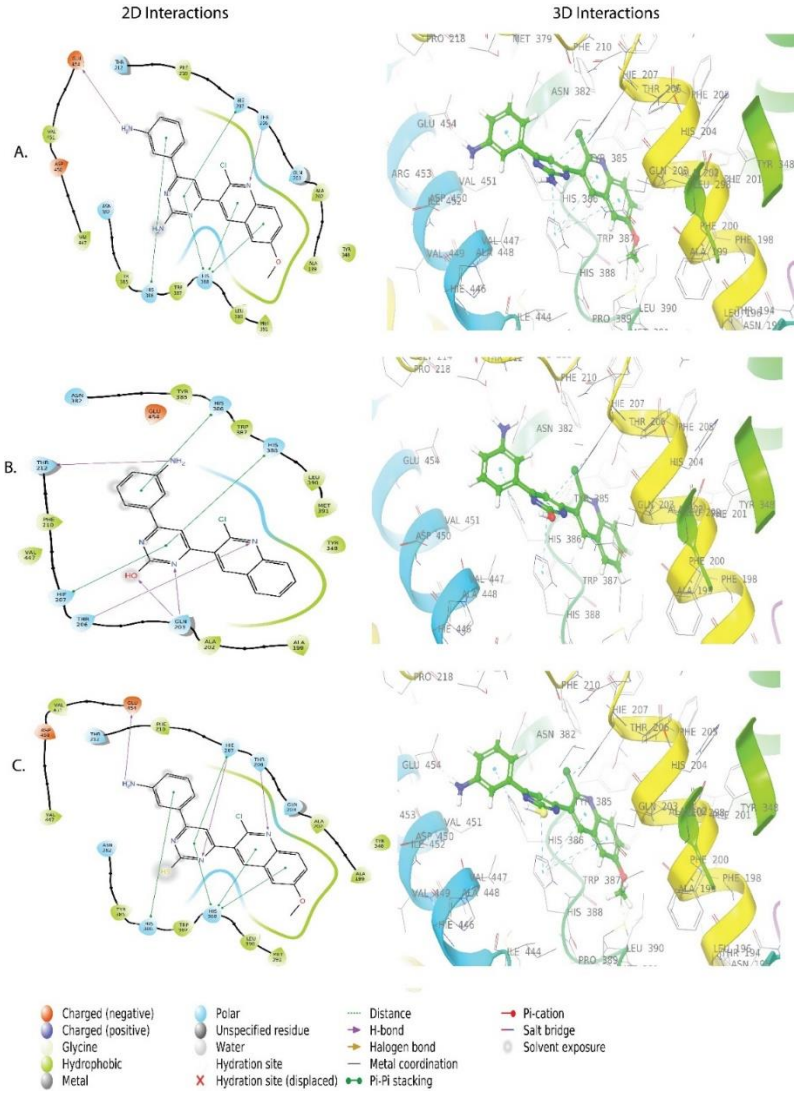

Fig. 2: 2D and 3D interaction of compound (A) QPDG5 with 6Y3C, (B) QPDU1 with 6Y3C, (C) QPDT5 with 6Y3C

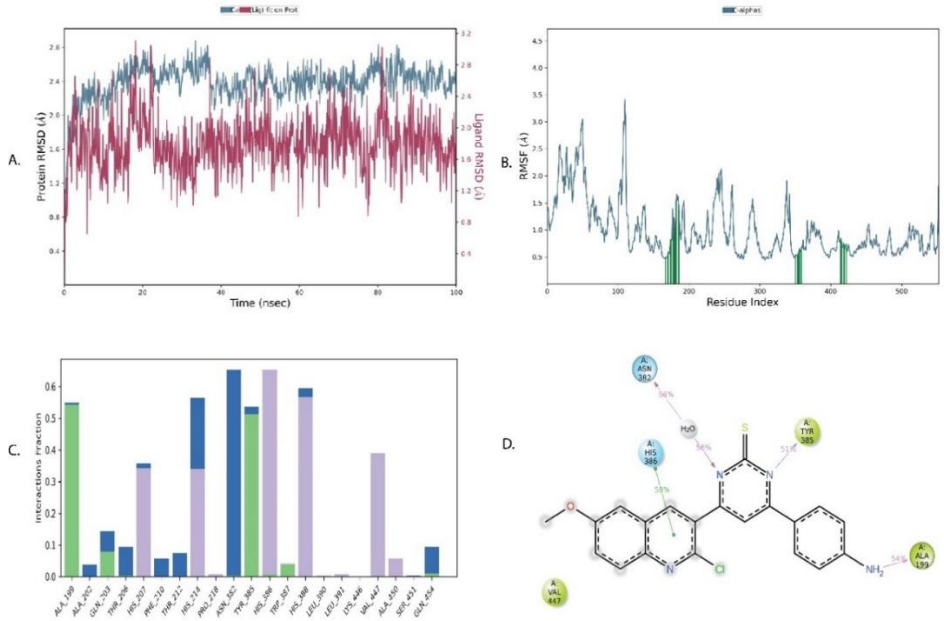

Fig. 3: MD simulation analysis of QPDT6 in complex with enzyme 5IKR (A) Protein-ligand RMSD (B) Protein RMSF (C) Protein-ligand contacts (D) Ligand-protein contacts

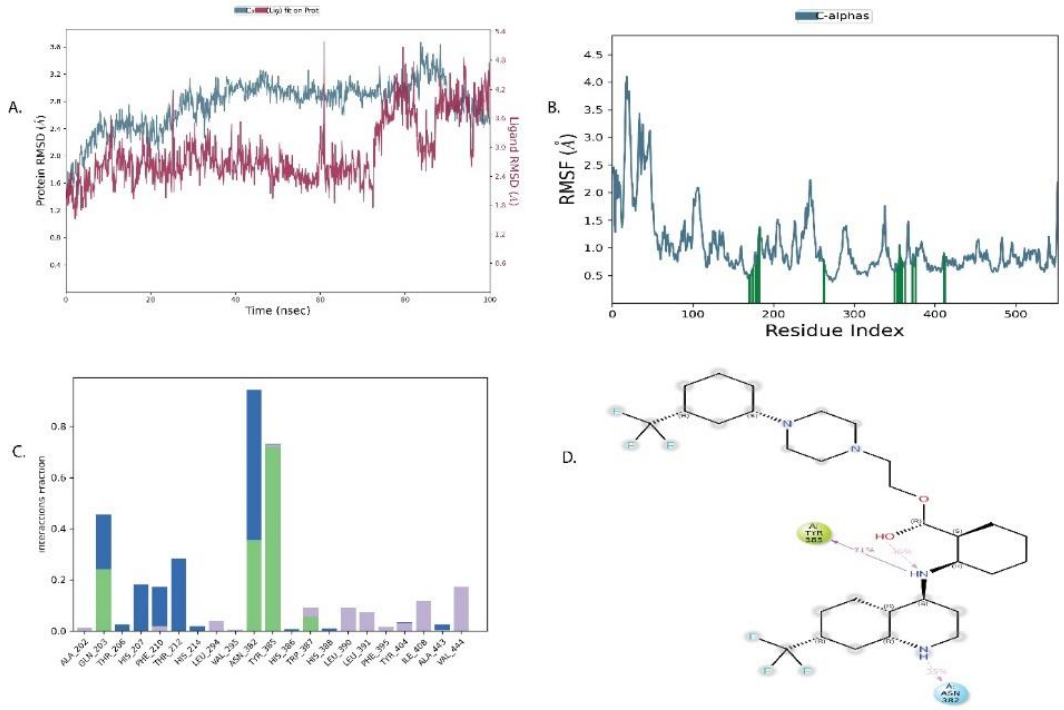

Fig. 4: MD simulation analysis of Antrafenine in complex with enzyme 5IKR (A) Protein-ligand RMSD (B) Protein RMSF (C) Protein-ligand contacts (D) Ligand-protein contacts

RMSD, RMSF, protein-ligand contact mapping, and ligand-protein contacts were analyzed for the standard drug Antrafenine during MD simulation and it is given in fig. 4.

DISCUSSION

Bioavailability is crucial for a compound to elicit a biological response, as poor bioavailability leads to ineffectiveness. Predicting pharmacokinetic parameters before drug development is essential to optimize compounds and reduce costs. Therefore, studying molecular parameters is vital [52]. The *in silico* ADMET studies of the quinoline derivatives, revealed that all the developed compounds exhibit excellent pharmacokinetic characteristics, Furthermore, these compounds demonstrated a tolerable toxicity profile, aligning with favorable drug-like properties. All pharmacokinetic parameters of the quinoline-based derivatives were found to be within the acceptable range [53].

Similarly, this study assessed the physicochemical and ADMET properties of designed compounds. The molecular weights of all the designed quinoline-linked pyrimidine derivatives, which range from 321.765 to 399.297, are less than 500. The log P values are less than five ranging from 3.104-4.976. Lipinski's rule of five is satisfied by the compounds because they have an appropriate number of hydrogen bond donors (less than five), acceptors (less than ten), log P, and molecular weight, which is consistent with experimental standards. Designed compounds showed a high percentage of human oral absorption, above 88%. QPDT series compounds showed great apparent Caco-2 cell permeability and apparent MDCK cell permeability; the values for the other series are within the recommended limit. Brain/blood partition coefficient and predicted binding to human serum albumin values are within the recommended range.

By using the Osiris property explorer, the molecules can be anticipated according to their functional groups. The results are displayed in three different colors: red, yellow, and green. The color red denotes a high danger of toxicity, yellow is a medium risk, and green is a low risk. The results suggest that all the compounds showed green color and they are safe and do not exhibit any toxicity in terms of carcinogenicity, mutagenicity, irritability, or harm to the reproductive system. The compounds possess acceptable drug scores.

Molecular docking studies were performed to determine the *in silico* anti-inflammatory activity of developed compounds. A molecular docking study for quinoline-incorporated pyrazole derivatives and Quinoline-2-Carboxamides was carried out on the COX-2 binding pocket. These compounds showed good binding characteristics and anti-inflammatory action within the COX-2 active site [54, 55]. Likewise, in the present study, COX enzymes were selected as targets. X-ray crystal structures of COX-2 (PDB ID: 5IKR) and COX-1 (PDB ID: 6Y3C) were obtained from the protein data bank.

In the QPDG series, compound QPDG3 showed the highest docking score of-7.026kcal/mol with COX-2, and with COX-1, QPDG5 displayed the highest docking score (table 5). QPDG3 showed hydrogen bonding with His 207 and His 386 through nitrogen and amino group respectively. It also shows pi-pi stacking with His 207 through the quinoline ring (fig. 1A). QPDG5 showed hydrogen bonding with Glu 454 and Thr 206 through the amino group and nitrogen atom, respectively. It shows pi-pi stacking with Hie 207, His 388, and His 386 through aromatic rings (fig. 2A).

The compounds of the QPDU series, QPDU6, and QPDU1, have the highest docking scores with COX-2 and COX-1, respectively, at-7.366 and-7.483 kcal/mol (table 5). QPDU6 showed hydrogen bonding with Ala 199 and Asn 382 through amino and hydroxyl groups, respectively. It also showed pi-pi stacking with His 388, His 386, and His 207 through aromatic rings and halogen bond with Gln 203 and His 207 via chloride group on the quinoline ring (fig. 1B). QPDU1 showed hydrogen bonding with Thr 212 and Thr 206 via amino group and nitrogen atom respectively. It also showed two more hydrogen bonds with Gln 203 through the nitrogen atom and hydroxyl group of the pyrimidine ring. Pi-pi stacking was observed with His 386, his 388, and Hie 207 through aromatic rings (fig. 2B).

QPDT6 and QPDT5 in the QPDT series compound demonstrated the highest docking scores, respectively, of-7.609 kcal/mol and-7.132 kcal/mol with COX-2 and COX-1 (table 5). QPDT6 showed hydrogen bonding with Ala 199, Asn 382, Pi-pi stacking with His 388, His 207 and halogen bonding with His 207, Gln 203 (fig. 1C) QPDT5 showed

hydrogen bonding with Glu 454, Hie 207, Thr 206 and pi-pi stacking with His 386, His 388, Hie 207 (fig. 2C).

The binding free energy of the protein-ligand complexes was found to verify the docking studies of the lead compound. The stability of a specific protein-ligand combination is determined by the binding energy (ΔG bind) released during bond formation, or rather, while the ligand and protein are interacting. All the compounds showed good binding-free energy, with values that ranged from-25.89 to-67.67 kcal mol−1 with COX-2 (table 6). The binding-free energy with COX-1 is between the range of-65.40 to-75.94 kcal mol−1 (table 7). The compounds QPDT7 and QPDT8 showed the highest binding free energy with COX-2 and COX-1 correspondingly.

The stability of compound QPDT6 in a complex with 5IKR was analyzed by performing MD simulations. An essential component of the MD simulation pathway that anticipates Cα variation in a dynamic environment is the protein Cα RMSD. There are not many fluctuations in the RMSD value of protein and ligand. Thus, it remains stable during the simulation. If the ligand's RMSD value is less than the protein's RMSD, it means that the ligand hasn't disseminated from its original binding site (fig. 3A). For every protein residue, the average variation from the starting point is calculated using RMSF. The RMSF identifies a particular protein structural element that departs from the average. The stability of protein molecules coupled to small molecules can be assessed using the RMSF of individual amino acids. The RMSF of each amino acid in the 5IKR protein coupled to compound QPDT6 is shown in fig 3B. QPDT6 interacts with 21 amino acids in the 5IKR. Most of the fluctuations are less than 2 A°, hence the residues are stable. The fluctuations are very low for most of the residues interacting with ligands. Which suggests that during the simulation, the interactions are quite stable. How the ligand and protein interacted was observed during the simulation. Within the time frame that has been set, Asn 382 forms water bridges, His 386 forms hydrophobic interaction for the majority of the time and it also forms water bridges for a very short period. Fig. 3C illustrates the specific sequence relationships amongst the various amino acid residues present in the complex QPDT6–5IKR. An illustration of detailed interactions of QPDT6 with the 5IKR residues is shown in fig. 3D. These interactions are stable for 51 – 58% of the simulation time.

CONCLUSION

In this study, we assessed the binding interactions of designed quinoline-linked pyrimidine derivatives with COX-1 and COX-2 enzymes using a thorough computational approach. The results of docking studies indicated that there were promising interactions between the ligands and the enzymes' active sites with QPDT6 showing the highest docking score. Using MD simulations, QPDT6's behavior was further investigated and its stability and conformational dynamics were demonstrated. Schrödinger's QikProp program was utilized to analyze the ADME properties. The results showed that quinoline derivatives have favorable physicochemical characteristics for drug-likeness, suggesting that they could be developed further as pharmaceutical agents. The compounds' toxicity properties were further investigated using Osiris Property Explorer and all the designed compounds were found to be safe. Additionally, the protein-ligand complexes' binding free energy was ascertained using the MM-GBSA approach, which offered crucial information regarding the strength of their interactions. The proposed compounds exhibit strong binding affinities to COX enzymes, stable interactions in MD simulations, and favorable drug-like features. These results lend support to the need for more research and development of these substances as possible anti-inflammatory drugs. To verify these compounds' safety and efficacy profiles, more research is required for synthesizing these compounds and *in vitro* and *in vivo* testing.

ACKNOWLEDGMENT

The authors are thankful to the authorities of NGSM Institute of Pharmaceutical Sciences, Nitte (Deemed to be University), Mangalore, India for providing all the necessary facilities.

FUNDING

Nil

AUTHORS CONTRIBUTIONS

Jennifer Fernandes and Manjunath S. Katagi contributed to the conception of the work, design of the work, and reviewed the manuscript. Deepthi K performed the experimental work, interpretation of data, and drafting of the manuscript. Sheshagiri Dixit and Deepshikha Singh contributed to the MD simulation study and result analysis. The final draft that was submitted for publication has been read and approved by all the authors.

CONFLICT OF INTERESTS

The authors declare no conflict of interest.

REFERENCES

1. Baranwal J, Kushwaha S, Singh S, Jyoti A. A review on the synthesis and pharmacological activity of heterocyclic compounds. Curr Phys Chem. 2023;13(1):2-19. doi: 10.2174/1877946813666221021144829.
2. Yadav P, Shah K. Quinolines, a perpetual, multipurpose scaffold in medicinal chemistry. Bioorg Chem. 2021;109:104639. doi: 10.1016/j.bioorg.2021.104639, PMID 33618829.
3. Kaur R, Kumar K. Synthetic and medicinal perspective of quinolines as antiviral agents. Eur J Med Chem. 2021;215:113220. doi: 10.1016/j.ejmech.2021.113220.
4. Kharb R, Kaur H. Therapeutic significance of quinoline derivatives as antimicrobial agents. Int Res J Pharm. 2013;4(3):63-9. doi: 10.7897/2230-8407.04311.
5. Singh SK, Singh S. A brief history of quinoline as antimalarial agents. Int J Pharm Sci Rev Res. 2014;25(1):295-302.
6. Coa JC, Castrillón W, Cardona W, Carda M, Ospina V, Muñoz JA. Synthesis, leishmanicidal, trypanocidal and cytotoxic activity of quinoline-hydrazone hybrids. Eur J Med Chem. 2015;101:746-53. doi: 10.1016/j.ejmech.2015.07.018, PMID 26218652.
7. Ilakiyalakshmi M, Arumugam Napoleon A. Review on recent development of quinoline for anticancer activities. Arab J Chem. 2022;15(11). doi: 10.1016/j.arabjc.2022.104168.
8. Khalifa NM, Al-Omar MA, Abd El-Galil AA, Abd El-Reheem M. Anti-inflammatory and analgesic activities of some novel carboxamides derived from 2-phenyl quinoline candidates. Biomed Res. 2017;28(2):869-74.
9. Mahajan P, Nikam M, Asrondkar A, Bobade A, Gill C. Synthesis, antioxidant, and anti-inflammatory evaluation of novel thiophene-fused quinoline based β-diketones and derivatives. J Heterocycl Chem. 2017;54(2):1415-22. doi: 10.1002/jhet.2722.
10. Mandewale MC, Patil UC, Shedge SV, Dappadwad UR, Yamgar RS. A review on quinoline hydrazone derivatives as a new class of potent antitubercular and anticancer agents. Beni Suef Univ J Basic Appl Sci. 2017;6(4):354-61. doi: 10.1016/j.bjbas.2017.07.005.
11. Das P, Deng X, Zhang L, Roth MG, Fontoura BM, Phillips MA. SAR-based optimization of a 4-quinoline carboxylic acid analog with potent anti-viral activity. ACS Med Chem Lett. 2013;4(6):517-21. doi: 10.1021/ml300464h, PMID 23930152.
12. Dorababu A. Recent update on antibacterial and antifungal activity of quinoline scaffolds. Arch Pharm. 2021;354(3):e2000232. doi: 10.1002/ardp.202000232, PMID 33210348.
13. Mouscadet JF, Desmaële D. Chemistry and structure-activity relationship of the styryl quinoline-type HIV integrase inhibitors. Molecules. 2010;15(5):3048-78. doi: 10.3390/molecules15053048, PMID 20657464.
14. Zajdel P, Marciniec K, Maslankiewicz A, Grychowska K, Satała G, Duszynska B. Antidepressant and antipsychotic activity of new quinoline- and isoquinoline-sulfonamide analogs of aripiprazole targeting serotonin 5-HT_1A/5-HT_2A/5-HT_7 and dopamine D_2/D_3 receptors. Eur J Med Chem. 2013;60:42-50. doi: 10.1016/j.ejmech.2012.11.042, PMID 23279866.
15. Wei CX, Deng XQ, Chai KY, Sun ZG, Quan ZS. Synthesis and anticonvulsant activity of 1-formamide-triazolo[4,3-a]quinoline derivatives. Arch Pharm Res. 2010;33(5):655-62. doi: 10.1007/s12272-010-0502-0.
16. Kumar A, Kumar P, Shetty CR, James JP, Shetty HC. Synthesis, antidiabetic evaluation and bioisosteric modification of

quinoline incorporated 2-pyrazoline derivatives. Indian J Pharm Educ Res. 2021;55(2):574-80. doi: 10.5530/ijper.55.2.96.

17. Cai Z, Zhou W, Sun L. Synthesis and HMG CoA reductase inhibition of 4-thiophenyl quinolines as potential hypocholesterolemic agents. Bioorg Med Chem. 2007;15(24):7809-29. doi: 10.1016/j.bmc.2007.08.044, PMID 17851082.
18. Gupta SK, Mishra A. Synthesis, characterization and screening for the anti-inflammatory and analgesic activity of quinoline derivatives bearing azetidinones scaffolds. Antiinflamm Antiallergy Agents Med Chem. 2016;15(1):31-43. doi: 10.2174/1871523015666160210124545, PMID 26860581.
19. Wang XQ, Zhao CP, Zhong LC, Zhu DL, Mai DH, Liang MG. Preparation of 4-flexible amino-2-arylethenyl-quinoline derivatives as multi-target agents for the treatment of Alzheimer's disease. Molecules. 2018;23(12):3100. doi: 10.3390/molecules23123100, PMID 30486440.
20. Sashidhara KV, Avula SR, Mishra V, Palnati GR, Singh LR, Singh N. Identification of quinoline-chalcone hybrids as potential antiulcer agents. Eur J Med Chem. 2015;89:638-53. doi: 10.1016/j.ejmech.2014.10.068, PMID 25462272.
21. Sharma V, Chitranshi N, Agarwal AK. Significance and biological importance of pyrimidine in the microbial world. Int J Med Chem. 2014;2014(1):202784. doi: 10.1155/2014/202784, PMID 25383216.
22. Kalčic F, Kolman V, Ajani H, Zídek Z, Janeba Z. Polysubstituted pyrimidines as mPGES-1 Inhibitors: discovery of potent inhibitors of PGE2 production with strong anti-inflammatory effects in carrageenan-induced rat paw edema. ChemMedChem. 2020;15(15):1398-407. doi: 10.1002/cmdc.202000258, PMID 32410351.
23. Abd El-Aleam RH, George RF, Hassan GS, Abdel-Rahman HM. Synthesis of 1,2,4-triazolo[1,5-a]pyrimidine derivatives: antimicrobial activity, DNA Gyrase inhibition and molecular docking. Bioorg Chem. 2020;94:103411. doi: 10.1016/j.bioorg.2019.103411.
24. Kumar B, Sharma P, Gupta VP, Khullar M, Singh S, Dogra N. Synthesis and biological evaluation of pyrimidine bridged combretastatin derivatives as potential anticancer agents and mechanistic studies. Bioorg Chem. 2018;78:130-40. doi: 10.1016/j.bioorg.2018.02.027, PMID 29554587.
25. Huang B, Kang D, Tian Y, Daelemans D, De Clercq E, Pannecouque C. Design, synthesis, and biological evaluation of piperidinyl-substituted [1,2,4]triazolo[1,5-a]pyrimidine derivatives as potential anti-HIV-1 agents with reduced cytotoxicity. Chem Biol Drug Des. 2021;97(1):67-76. doi: 10.1111/cbdd.13760, PMID 32725669.
26. Bruno O, Schenone S, Ranise A, Bondavalli F, Barocelli E, Ballabeni V. New polycyclic pyrimidine derivatives with antiplatelet *in vitro* activity: synthesis and pharmacological screening. Bioorg Med Chem. 2001;9(3):629-36. doi: 10.1016/s0968-0896(00)00272-8, PMID 11310597.
27. Farghaly AM, Aboul Wafa OM, Elshaier YA, Badawi WA, Haridy HH, Mubarak HA. Design, synthesis, and antihypertensive activity of new pyrimidine derivatives endowing new pharmacophores. Med Chem Res. 2019;28(3):360-79. doi: 10.1007/S00044-019-02289-6.
28. Farghaly TA, Harras MF, Alsaedi AM, Thakir HA, Mahmoud HK, Katowah DF. Antiviral activity of pyrimidine containing compounds: patent review. Mini Rev Med Chem: Patent Review. 2023;23(7):821-51. doi: 10.2174/1389557523666221220142911, PMID 36545712.
29. Wu W, Lan W, Wu C, Fei Q. Synthesis and antifungal activity of pyrimidine derivatives containing an amide moiety. Front Chem. 2021;9:695628. doi: 10.3389/fchem.2021.695628, PMID 34322475.
30. Pant S, Kumar K R, Rana P, Anthwal T, Ali SM, Gupta M et al. Novel substituted pyrimidine derivatives as potential anti-alzheimer's agents: synthesis, biological, and molecular docking studies. ACS Chem Neurosci. 2024;15(4):783-97. doi: 10.1021/acschemneuro.3c00662, PMID 38320262.
31. Gupta A, Bhat HR, Singh UP. Discovery of novel hybrids of Morpholino-1,3,5-triazine-pyrimidine as an anti-diabetic agent in High-fat, Low-dose Streptozotocin-induced diabetes in wistar rats: an *in vitro*, in silico and *in vivo* study. J Mol Struct. 2023;1294:136478. doi: 10.1016/j.molstruc.2023.136478.
32. Liu P, Yang Y, Tang Y, Yang T, Sang Z, Liu Z. Design and synthesis of novel pyrimidine derivatives as potent antitubercular agents. Eur J Med Chem. 2019;163:169-82. doi: 10.1016/j.ejmech.2018.11.054, PMID 30508666. ejmech.2018.11.054.
33. Nair N, Majeed J, Pandey PK, Sweety R, Thakur R. Antioxidant potential of pyrimidine derivatives against oxidative stress. Indian J Pharm Sci. 2022;84(1):14-26. doi: 10.36468/pharmaceutical-sciences.890.
34. Mathew B, Suresh J, Anbazhagan S. Development of novel (1- H) benzimidazole bearing pyrimidine-trione based MAO-A inhibitors: Synthesis, docking studies and antidepressant activity. J Saudi Chem Soc. 2016;20:S132-9, doi: 10.1016/j.jscs.2012.09.015.
35. Arora N, Pandeya SN. Synthesis and analgesic activity of novel pyrimidine derivatives. Synthesis. 2011;11(1):48-52.
36. Mohana KN, Prasanna Kumar BN, Mallesha L. Synthesis and biological activity of some pyrimidine derivatives. Drug Invent Today. 2013;5(3):216-22. doi: 10.1016/j.dit.2013.08.004.
37. Kumar B, Kumar M, Dwivedi AR, Kumar V. Synthesis, Biological Evaluation and Molecular Modeling Studies of Propargyl-Containing 2,4,6-Trisubstituted Pyrimidine Derivatives as Potential Anti-Parkinson Agents. ChemMedChem. 2018;13(7):705-12. doi: 10.1002/cmdc.201700589, PMID 29534334.
38. Jain KS. A Novel 2, 4-dihalothieno [2, 3-d] pyrimidine as an antihyperlipidemic agent: synthesis, biological evaluation and investigation into its mechanism of action. EC Pharmacol Toxicol. 2019;7:125-43.
39. Chandana L, Bhikshapathi DV. Ethnopharmacological investigation of *Pleurotus ostreatus* for anti-oxidative and anti-inflammatory activity in experimental animals. Asian J Pharm Clin Res. 2024;17(4):37-41. doi: 10.22159/ajpcr.2024.v17i4.49533.
40. Chen L, Deng H, Cui H, Fang J, Zuo Z, Deng J. Inflammatory responses and inflammation-associated diseases in organs. Oncotarget. 2018;9(6):7204-18. doi: 10.18632/oncotarget.23208, PMID 29467962.
41. El-Sharief MA, Abbas SY, El-Sharief AM, Sabry NM, Moussa Z, El-Messery SM. 5-Thioxoimidazolidine-2-one derivatives: synthesis, anti-inflammatory activity, analgesic activity, COX inhibition assay and molecular modelling study. Bioorg Chem. 2019;87:679-87. doi: 10.1016/j.bioorg.2019.03.075, PMID 30953887.
42. Dvorakova M, Langhansova L, Temml V, Pavicic A, Vanek T, Landa P. Synthesis, inhibitory activity, and *in silico* modeling of selective COX-1 inhibitors with a quinazoline core. ACS Med Chem Lett. 2021;12(4):610-6. doi: 10.1021/acsmedchemlett.1c00004, PMID 33854702.
43. Hawash M, Jaradat N, Hameedi S, Mousa A. Design, synthesis and biological evaluation of novel benzodioxole derivatives as COX inhibitors and cytotoxic agents. BMC Chem. 2020;14(1):54. doi: 10.1186/s13065-020-00706-1, PMID 32944715.
44. Cardinal S, Paquet Cote PA, Azelmat J, Bouchard C, Grenier D, Voyer N. Synthesis and anti-inflammatory activity of isoquebecol. Bioorg Med Chem. 2017;25(7):2043-56. doi: 10.1016/j.bmc.2017.01.050, PMID 28258800.
45. Dhawale S, Gawale S, Jadhav A, Gethe K, Raut P, Hiwarale N. *In silico* approach targeting polyphenol as FabH inhibitor in bacterial infection. Int J Pharm Pharm Sci. 2022;14(11):25-30. doi: 10.22159/ijpps.2022v14i11.45816.
46. Jays J, Saravanan J. A molecular modelling approach for structure-based virtual screening and identification of novel isoxazoles as potential antimicrobial agents against *S. aureus*. Int J Pharm Pharm Sci. 2024;16(4):36-41. doi: 10.22159/ijpps.2024v16i4.49731.
47. Elmi A, Sayem SA, Ahmed M, Abdoul-Latif F. Natural compounds from djiboutian medicinal plants as inhibitors of covid-19 by *in silico* investigations. Int J Curr Pharm Sci. 2020;12(4):52-7. doi: 10.22159/ijcpr.2020v12i4.39051.
48. Chand J, Kandy AT, Prasad K, Mathew J, Sherin F, Subramanian G. *In silico*, preparation and *in vitro* studies of benzylidene-based

hydroxy benzyl urea derivatives as free radical scavengers in Parkinson's disease. Int J App Pharm. 2024;16(3):217-24. doi: 10.22159/ijap.2024v16i3.50628.

49. Sachdeo R, Khanwelkar C, Shete A. *In silico* exploration of berberine as a potential wound healing agent via network pharmacology, molecular docking, and molecular dynamics simulation. Int J App Pharm. 2024;16(2):188-94. doi: 10.22159/ijap.2024v16i2.49922.
50. Zafirah Ismail N, Annamalai N, Mohamad Zain NN, Arsad H. Molecular docking of selected compounds from *Clinacanthus nutans* with BCL-2, p53, caspase-3 and caspase-8 proteins in the apoptosis pathway. J Biol Sci Opin. 2020;8(1):4-11. doi: 10.7897/2321-6328.081119.
51. Baqi MA, Jayanthi K, R. Identification of benzylidene amino phenol inhibitors targeting thymidylate kinase for colon cancer treatment through *in silico* studies. Int J App Pharm. 2024;16(4):92-9. doi: 10.22159/ijap.2024v16i4.50874.
52. Mahantheshappa SS, Shivanna H, Satyanarayan ND. Synthesis, antimicrobial, antioxidant, and ADMET studies of quinoline derivatives. Eur J Chem. 2021;12(1):37-44. doi: 10.5155/eurjchem.12.1.37-44.2038.
53. Mhaske GS, Thorat SR, Pawar VS, Pawar RS, Jambhulkar SR, Ghumre OA. Computational Molecular Docking and In-Silico, ADMET Prediction Studies of Quinoline Derivatives as EPHB4 Inhibitor. Curr Indian Sci. 2024;02:1-16, doi: 10.2174/012210299X265033240116113623.
54. El-Feky SA, Abd El-Samii ZK, Osman NA, Lashine J, Kamel MA, Thabet HKh. Synthesis, molecular docking and anti-inflammatory screening of novel quinoline-incorporated pyrazole derivatives using the Pfitzinger reaction II. Bioorg Chem. 2015;58:104-16. doi: 10.1016/j.bioorg.2014.12.003. PMID 25590381.
55. Abdelrahman MH, Youssif BG, Abdelgawad MA, Abdelazeem AH, Ibrahim HM, Moustafa AE. Synthesis, biological evaluation, docking study and ulcerogenicity profiling of some novel quinoline-2-carboxamides as dual COXs/LOX inhibitors endowed with anti-inflammatory activity. Eur J Med Chem. 2017;127:972-85. doi: 10.1016/j.ejmech.2016.11.006, PMID 27837994.